Smart Mater. Struct. 5 (1996) 796–800. Printed in the UK

Continuous carbon fibre epoxy-matrix composite as a sensor of its own strain

Xiaojun Wang and D D L Chung

Composite Materials Research Laboratory, State University of New York at Buffalo, Buffalo, NY 14260-4400, USA

Received 15 December 1995, accepted for publication 28 June 1996

Abstract. Unidirectional continuous carbon fibre reinforced epoxy was found to be able to sense its own strain in the fibre direction, due to its longitudinal electrical resistance decreasing reversibly and its transverse resistance increasing reversibly upon longitudinal tension. The strain sensitivity (gauge factor) is from −35.7 to −37.6 and from +34.2 to +48.7 for the longitudinal and transverse resistances respectively. Both effects originate from resistivity changes associated with the increase in the degree of fibre alignment upon longitudinal tension. Either effect allows strain sensing. Slight irreversibility is associated with the resistance decreasing after the first strain cycle and stems from the decrease in the degree of neatness of the fibre arrangement.

1. Introduction

Strain sensing during static and dynamic loading is needed for aerospace structures, civil infrastructure systems, as well as machinery. In particular, the ability to sense strain under dynamic loading allows dynamic load monitoring in real time. Strain sensing differs from damage sensing, as strain can be reversible, whereas damage is irreversible. Reversible strain can only be sensed in real time, whereas damage does not have to be sensed in real time. Therefore, reversible strain sensing is usually more challenging than damage sensing.

The sensing of strain in a structure is commonly achieved by attaching to or embedding in the structure one or more strain sensors, which can be piezoresistive, piezoelectric or other types of sensors. For the case of a structure made of continuous carbon fibre reinforced epoxy (a composite commonly used in aerospace structures), the strain sensors are commonly embedded between the fibre layers during composite fabrication. The embedded sensors are intrusive and tend to degrade the mechanical properties of the composite. Attached sensors are intrusive and tend to degrade the mechanical properties of the composite. Attached sensors are less intrusive, but they are not durable. In this work, instead of using attached or embedded sensors, we used the continuous carbon fibre reinforced epoxy itself as the sensor. In other words, the structure material is itself a sensor, so that the structure is smart everywhere. In contrast, a structure with embedded or attached sensors is only smart in the vicinity of each sensor.

The electrical resistance of a single carbon fibre increases reversibly upon tension, such that the fractional reversible increase in resistance ($\Delta R/R_0$) per unit strain (i.e. the strain sensitivity or the gauge factor) is 1.3–1.7 [1]. For the carbon used in this work, the strain sensitivity is 1.8, the effect is mostly due to dimensional change rather than resistivity change and the resistance change is totally reversible when the stress is below half of the fracture stress [2]. The electrical resistivity of a short carbon fibre epoxy-matrix composite increases reversibly upon tension (with strain sensitivity 6–23) due to increase of the distance between adjacent fibres and decreases reversibly upon compression (with strain sensitivity 29–31) due to decrease of the distance between adjacent fibres [3]. This paper addresses the strain sensing ability of an epoxy-matrix composite with continuous unidirectional carbon fibres, as such composites are widely used in aerospace structures, whereas short carbon fibre composites are not suitable for structural applications. Previous related work on continuous carbon fibre composites pertains mainly to damage sensing rather than strain sensing, as it makes use of the irreversible increase in electrical resistivity upon breakage of the fibres at tension [4, 5].

2. Experimental method

Composite samples were constructed from individual layers cut from a 30.5 cm wide unidirectional carbon fibre prepreg tape manufactured by ICI Fiberite (Tempe, AZ). The product used was Hy-E 1076E, which consisted of a 976 epoxy matrix and 10E carbon fibres. The fibre and matrix properties are shown in table 1.

The composite laminates were laid up in a (10.2 × 17.8 cm^2 (4 × 7 in^2) platten compression mould with

0964-1726/96/060796+05$19.50

Table 1. Carbon fibre and epoxy matrix properties (according to ICI Fiberite).

Torayca T-300 (6 K) untwisted, UC-309 sized	
Density	1.76 g cm^{-3}
Tensile modulus	221 GPa
Tensile strength	3.1 GPa
Epoxy	
Process temperature	350 °F (177 °C)
Maximum service temperature	350 °F (177 °C) dry 250 °F (121 °C) wet
Flexural modulus	3.7 GPa
Flexural strength	138 MPa
T_g	232 °C
Density	1.28 g cm^{-3}

laminate configuration [0]. The individual 4 × 7 in^2 fibre layers (14 per laminate) were cut from the prepreg tape. The layers were stacked in the mould with a mould release film on the top and bottom of the lay-up. No liquid mould release was used. The laminates were cured using a cycle based on the ICI Fiberite C-5 cure cycle. Curing occurred at 355 ± 10 °F (179 ± 6 °C) and 89 psi (0.61 MPa) for 120 min. The laminates were then cut into pieces of size 160 × 14 mm^2. The density and nominal thickness of the laminate were 1.52 ± 0.01 g cm^{-3} and 1.4 mm respectively after curing. The exact thickness of each specimen cut from the laminate was separately measured in order to determine the longitudinal and transverse resistivities and the longitudinal modulus of the specimen. The volume fraction of carbon fibres in the composite was 58%. Glass fibre reinforced epoxy end tabs were applied to both ends on both sides of each cured piece, such that each tab was 30 mm long and the inner edges of the end tabs on the same side were 100 mm apart and the outer edges were 160 mm apart.

The volume electrical resistance R was measured using the four-probe method while cyclic tension was applied in the longitudinal direction. Silver paint was used for all electrical contacts. The four probes consisted of two outer current probes and two inner voltage probes. The resistance R refers to the sample resistance between the inner probes. Longitudinal and transverse R values were measured in different samples. For the longitudinal R measurement, the four electrical contacts were around the whole perimeter of the sample in four parallel planes that were perpendicular to the stress axis, such that the inner probes were 60 mm apart and the outer probes were 78 mm apart. For the transverse R measurement, the current contacts were centred on the largest opposite faces and in the form of open rectangles of length 70 mm in the longitudinal direction, while each of the two voltage contacts was in the form of a solid rectangle (of length 20 mm in the longitudinal direction) surrounded by a current contact (open rectangle). Thus, each face had a current contact surrounding a voltage contact. A strain gauge was attached to the very centre of one of the largest opposite faces, for both longitudinal and transverse R measurement samples. In the case of the transverse R measurement sample, the strain gauge was at the centre of the inner rectangle (voltage contact). A Keithley 2001 multimeter was used. A hydraulic mechanical testing system (MTS 810) was used in the test to provide a displacement rate of 1.0 mm min^{-1}.

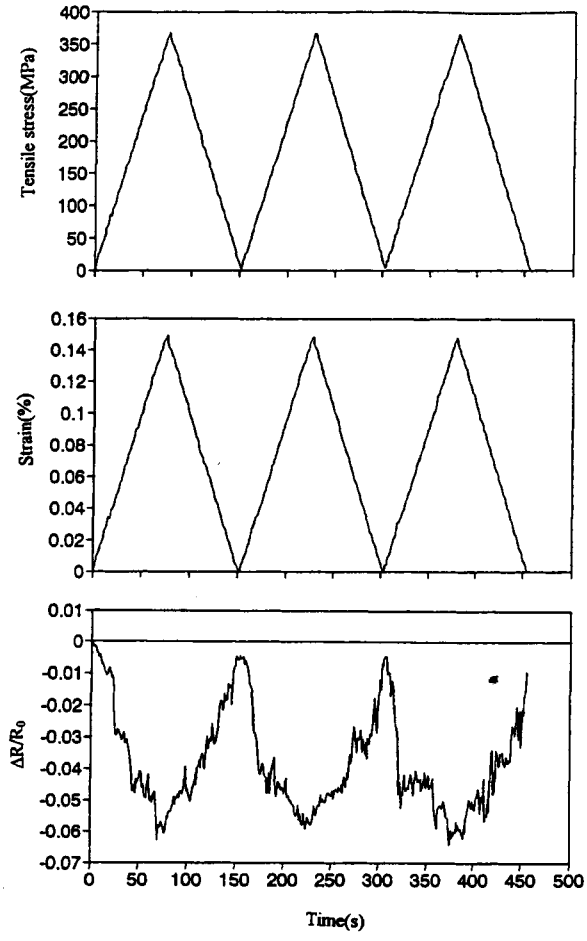

Figure 1. Longitudinal stress and strain and fractional resistance increase ($\Delta R/R_0$) obtained simultaneously during cyclic tension to a stress amplitude equal to 32% of the breaking stress.

3. Results

Figure 1 shows the longitudinal stress, strain and fractional longitudinal resistance increase (longitudinal $\Delta R/R_0$) obtained simultaneously during cyclic tension to a stress amplitude equal to 32% of the breaking stress. The strain returned to zero at the end of each cycle. Because of the small strains involved, $\Delta R/R_0$ is essentially equal to the fractional increase in resistivity. The longitudinal $\Delta R/R_0$ decreased upon loading and increased upon unloading in every cycle, such that R irreversibly decreased slightly after the first cycle (i.e. $\Delta R/R_0$ did not return to zero at the end of the first cycle). When the stress amplitude was raised to 36% of the breaking stress, the effect was similar, except that both the reversible and irreversible parts of $\Delta R/R_0$ were larger, as shown in table 2.

Figure 2 shows the longitudinal stress, strain and $\Delta R/R_0$ obtained simultaneously during static tensile loading up to fracture. The longitudinal $\Delta R/R_0$ first decreased and then increased in steps as the strain increased.

Table 2. Reversible and irreversible parts of $\Delta R/R_0$ and strain sensitivity in both longitudinal and transverse directions at various stress amplitudes.

	Maximum fracture stress	$\Delta R/R_0$ Reversible	$\Delta R/R_0$ Irreversible	Strain Sensitivity*
Longitudinal	32%	−0.050	−0.005	−35.7
	36%	−0.068	−0.012	−37.6
Transverse	35%	0.06	−0.017	34.2
	45%	0.11	−0.018	48.7

* Reversible $\Delta R/R_0$ divided by the longitudinal strain amplitude.

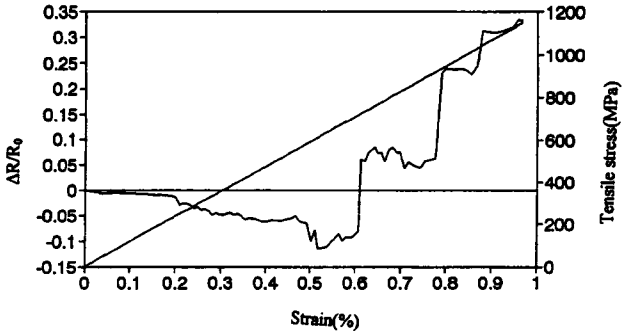

Figure 2. Longitudinal stress, strain and fractional resistance increase ($\Delta R/R_0$) obtained simultaneously during static tension up to fracture, which occurs at the highest strain in the curves. Full curve, $\Delta R/R_0$ versus strain; broken curve, tensile stress versus strain.

The decrease in $\Delta R/R_0$ in the low-strain regime is consistent with the trend shown in figure 1. The difference in the $\Delta R/R_0$ values at the same strain between figures 1 and 2 is due to the variation in the degree of fibre alignment from sample to sample within the same laminate. This variation is addressed later in this paper.

Figure 3 shows the longitudinal stress and strain and the transverse $\Delta R/R_0$ obtained simultaneously during cyclic tension to a stress amplitude equal to 35% of the breaking stress. As expected, the strain returned to zero at the end of each cycle. The transverse $\Delta R/R_0$ increased upon loading and decreased upon unloading in every cycle, such that R irreversibly decreased slightly after the first cycle (i.e. $\Delta R/R_0$ did not return to zero at the end of the first cycle). Upon increasing the stress amplitude to 45% of the breaking stress, the effect was similar, except that the reversible part of $\Delta R/R_0$ was larger, as shown in table 2.

Figure 4 shows the longitudinal stress and strain and transverse $\Delta R/R_0$ obtained simultaneously during static tensile loading up to fracture. The transverse $\Delta R/R_0$ first increased abruptly and then levelled off as the strain increased.

The strain sensitivity (gauge factor) is defined as the reversible part of $\Delta R/R_0$ divided by the longitudinal strain amplitude. It is negative for the longitudinal $\Delta R/R_0$ and positive for the transverse $\Delta R/R_0$, as shown in table 2. The magnitudes are comparable for the longitudinal and transverse strain sensitivities. As a result, whether the longitudinal R or the transverse R is preferred for strain sensing just depends on the convenience of electrical

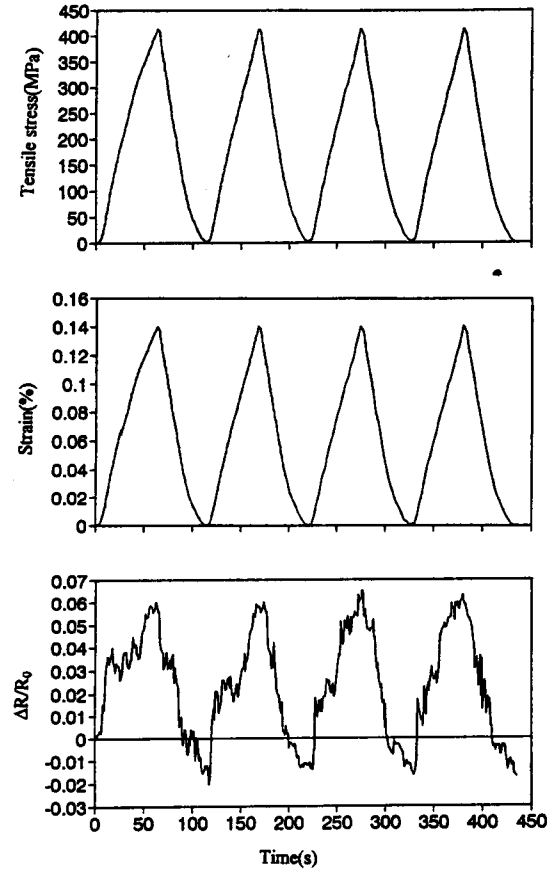

Figure 3. Longitudinal stress and strain and the transverse $\Delta R/R_0$ obtained simultaneously during cyclic tension to a stress amplitude equal to 35% of the breaking stress.

contact application for the geometry of the particular smart structure.

The tensile modulus was determined from the slope of the stress–strain curve in the elastic regime, as in the regimes shown in figures 1 and 3, for each sample that was tested electromechanically. Figure 5 shows that the absolute value of the reversible part of $\Delta R/R_0$ (both longitudinal and transverse) decreases with increasing tensile modulus. In other words, different samples were slightly different in the degree of fibre alignment, even though they were cut from the same laminate. Nevertheless, a sample with a larger absolute value of the reversible part of $\Delta R/R_0$ tended to have a smaller tensile modulus.

The electrical resistivity in the longitudinal and transverse directions under no load is shown in figures 6

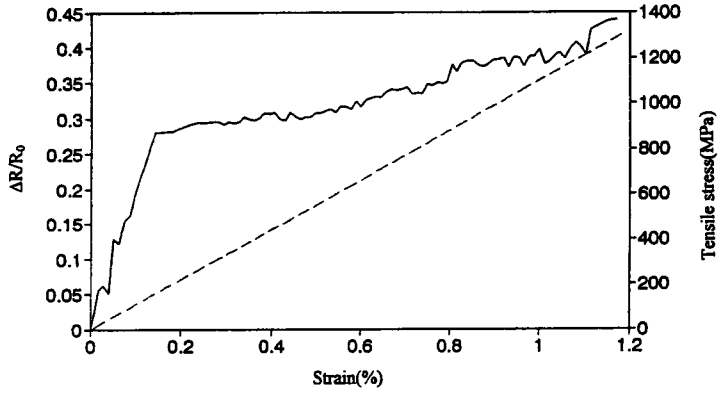

Figure 4. Longitudinal stress and strain and the transverse $\Delta R/R_0$ obtained simultaneously during static tension up to fracture, which occurs at the highest strain in the curves. Full curve, $\Delta R/R_0$ versus strain; broken curve, tensile stress versus strain.

and 7 respectively. Also shown in figures 6 and 7 is the absolute value of the reversible part of $\Delta R/R_0$ in the corresponding direction for each corresponding sample tested electromechanically. The absolute value of the reversible part of the longitudinal $\Delta R/R_0$ increases with longitudinal resistivity (figure 6), whereas the reversible part of the transverse $\Delta R/R_0$ decreases with increasing transverse resistivity (figure 7).

Results similar to those shown in figures 1–4 were obtained on similar composites obtained from different sources, though the magnitudes of the electromechanical effect varied, probably because of the variation of the inherent degree of fibre alignment—the smaller the inherent degree of fibre alignment, the larger was the effect.

Because of the low data acquisition rate, the strain at which the resistance starts to change could not be determined for the composite strain sensor of this work. Nevertheless, a longitudinal strain as low as 7×10^{-5} was detected by measuring the longitudinal $\Delta R/R_0$, and a longitudinal strain as low as 5×10^{-5} was detected by measuring the transverse $\Delta R/R_0$, using a data acquisition rate of 20 s^{-1}. By increasing the data acquisition rate, these upper bounds will be decreased.

4. Discussion

A dimensional change without any resistivity change would have caused R to increase during tensile loading. In contrast, R was observed to decrease (not increase) upon tensile loading. Furthermore, the observed magnitude of $\Delta R/R_0$ was 9–14 times that of $\Delta R/R_0$ calculated by assuming that $\Delta R/R_0$ was only due to dimensional change and not due to any resistivity change. Hence the contribution of $\Delta R/R_0$ from the dimensional change is negligible compared to that from the resistivity change.

From the longitudinal $\Delta R/R_0$, the strain sensitivity is -35.7 when the stress amplitude is 32% of the fracture stress and -37.6 when the stress amplitude is 36% of the fracture stress. The strain sensitivity is negative, in contrast to the positive values for a single carbon fibre [1] and for a short carbon fibre epoxy-matrix composite [3]. This difference means that the origin of the strain sensing ability of the continuous carbon fibre epoxy-matrix composite must be different from that of a single carbon fibre or that of a short fibre composite.

The decrease in longitudinal $\Delta R/R_0$ and increase in transverse $\Delta R/R_0$ upon longitudinal tension, as observed in this work for a continuous carbon fibre composite in cyclic loading (figures 1 and 3) or static loading at low strains (figures 2 and 4) are all attributed to the increase in the degree of alignment of the fibres upon longitudinal tension. The increase in the degree of alignment causes the longitudinal resistivity to decrease. In addition, it causes the adjacent fibre layers to have less chance of touching one another, so that transverse resistivity increases. The effects are almost totally reversible (figures 1 and 3), when the strain is reversible. That the reversible part of $\Delta R/R_0$ is due to the increase in the degree of alignment of the fibres upon longitudinal tension is supported by the facts that the longitudinal tensile modulus decreases with increasing magnitude of the irreversible part of $\Delta R/R_0$ (figure 5) and the longitudinal tensile modulus is known to decrease with decreasing degree of alignment of the fibres. In other words, the lower the degree of alignment of the fibres under no load, the greater the magnitude of the reversible part of $\Delta R/R_0$. Also consistent with the notion that the reversible part of $\Delta R/R_0$ is due to the increase in the degree of alignment of the fibres upon longitudinal tension is the observation that the absolute value of the reversible part of the longitudinal $\Delta R/R_0$ increases with increasing longitudinal resistivity at no load (figure 6), and that the reversible part of transverse $\Delta R/R_0$ decreases with increasing transverse resistivity at no load (figure 7), since the longitudinal resistivity is expected to decrease with increasing degree of fibre alignment while the transverse resistivity is expected to increase with increasing degree of fibre alignment.

The irreversible behaviour, though small compared to the reversible behaviour, is such that R (longitudinal or transverse) is irreversibly decreased after the first cycle. This behaviour is attributed to the irreversible disturbance to the fibre arrangement at the end of the first cycle, such that the fibre arrangement becomes less neat. A less neat fibre arrangement means more chance for the adjacent fibre layers to touch one another.

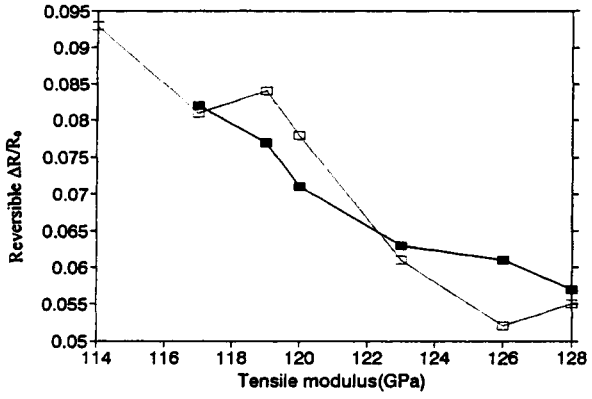

Figure 5. Variation of the absolute value of the reversible part of $\Delta R/R_0$ with the longitudinal tensile modulus. Full curve and full rectangles, longitudinal $\Delta R/R_0$, obtained at a fixed stress amplitude equal to 35% of the breaking stress. Broken curve and open rectangles, transverse $\Delta R/R_0$, obtained at a fixed stress amplitude equal to 30% of the breaking stress.

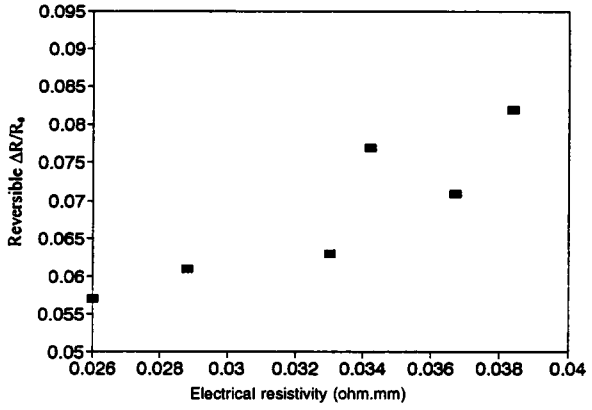

Figure 6. Variation of the absolute value of the reversible part of the longitudinal $\Delta R/R_0$ with the longitudinal resistivity at no load.

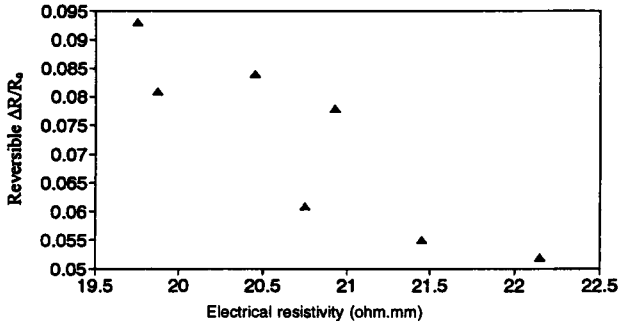

Figure 7. Variation of the reversible part of the transverse $\Delta R/R_0$ with transverse resistivity at no load.

The stepwise increase of the longitudinal $\Delta R/R_0$ in the large-strain regime (figure 2) is attributed to fibre breakage, which probably occurs in spurts. Such a stepwise increase has been observed previously and also attributed to fibre breakage [5].

The transverse $\Delta R/R_0$ increases abruptly at low strains but increases gradually at high strains (figure 4). This is because only a small change in the degree of fibre alignment causes a large change in the chance of adjacent fibre layers to touch one another, and the resistance changes abruptly with the separation between adjacent fibre layers at small separations but changes gradually with the separation at large separations. Moreover, fibre breakage, which occurs at high strains, essentially does not affect the transverse $\Delta R/R_0$ (figure 4), but affects the longitudinal $\Delta R/R_0$ (figure 2).

The electromechanical effect was observed only in unidirectional composites in this work. However, this effect is also present in multidirectional composites, which constitute the subject of a separate publication.

The magnitude of the tensile strain sensitivity (36–38) is higher than that (1.8) for a single carbon fibre [2] and that (6–23) for short carbon fibre epoxy-matrix composites [3]. However, it is lower than the value of up to 500 for short carbon fibre cement-matrix composites [6–8]. These differences in strain sensitivity are due to the differences in the origin of the sensing ability.

5. Conclusion

A new electromechanical effect was observed in unidirectional continuous carbon fibre reinforced epoxy. This effect allows the composite to serve as a sensor of its own strain in the fibre direction. The effect is such that the longitudinal $\Delta R/R_0$ decreases and the transverse $\Delta R/R_0$ increases upon longitudinal tension due to the increase in the degree of fibre alignment. The strain sensitivity (gauge factor) is large in magnitude (34–49). The effect is almost totally reversible when the longitudinal strain is reversible. The irreversible behaviour involves $\Delta R/R_0$ (longitudinal or transverse) decreasing irreversibly after the first cycle due to an irreversible decrease in the degree of neatness of the fibre arrangement.

References

[1] Conor P C and Owston C N 1969 *Nature* **223** 1146–7
[2] Wang X and Chung D D L 1996 *Carbon* at press
[3] Wang X and Chung D D L 1995 *Smart Mater. Struct.* **4** 363–7
[4] Muto N, Yanagida H, Nakatsuji T, Sugita M and Ohtsuka Y 1993 *J. Am. Ceram. Soc.* **76** 875–9
[5] Schulte K and Baron Ch 1989 *Composites Sci. Technol.* **36** 63–76
[6] Chen P-W and Chung D D L 1993 *Smart Mater. Struct.* **2** 22–30
[7] Chen P-W and Chung D D L 1995 *J. Am. Ceram. Soc.* **78** 816–8
[8] Chen P-W and Chung D D L 1996 *Composites* **27B** 11–23